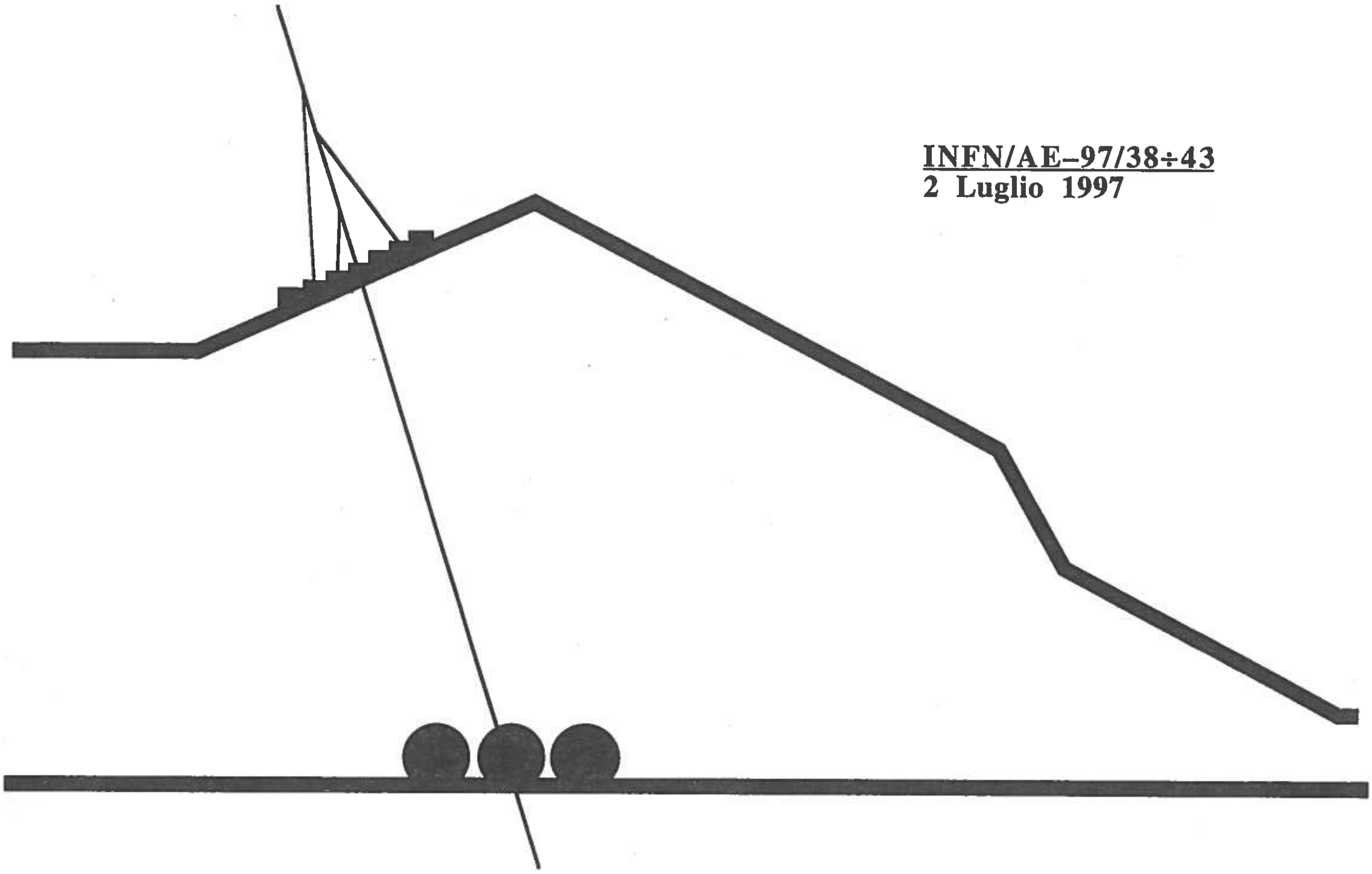

INFN/AE–97/38÷43
2 Luglio 1997

Contributions of the LVD Collaboration to the XXV ICRC
Durban, South Africa July 28–Aug. 10, 1997

INFN – Laboratori Nazionali del Gran Sasso

*Published by **SIS–Pubblicazioni***
dei Laboratori Nazionali di Frascati

EAS-TOP COLLABORATION

M.Aglietta[a,b], B.Alessandro[b], P.Antonioli[c], F.Arneodo[d,e], L.Bergamasco[b,f], M.Bertaina[b,f], C.Castagnoli[a,b], A.Castellina[a,b], A.Chiavassa[b,f], G.Cini Castagnoli[b,f], B.D'Ettorre Piazzoli[g], G.Di Sciascio[g], W.Fulgione[a,b], P.Galeotti[b,f], P.L.Ghia[b,f], M.Iacovacci[g], G.Mannocchi[a,b], C.Morello[a,b], G.Navarra[b,f], O.Saavedra[b,f], G.C.Trinchero[a,b], P.Vallania[a,b], S.Vernetto[a,b], C.Vigorito[b,f]

a) Istituto di Cosmo-Geofisica del CNR, Corso Fiume 4, 10133 Torino, Italy
b) Istituto Nazionale di Fisica Nucleare, Via Pietro Giuria 1, 10125 Torino, Italy
c) Istituto Nazionale di Fisica Nucleare, Via Irnerio 46, 40126 Bologna, Italy
d) Dipartimento di Fisica dell' Università dell'Aquila, Via Vetoio, 67010 L'Aquila, Italy
e) INFN Laboratori Nazionali del Gran Sasso, S.S. 17 bis, 67010 Assergi (AQ), Italy
f) Dipartimento di Fisica Generale dell' Università, Via P. Giuria, 1, 10125 Torino, Italy
g) Dipartimento di Scienze Fisiche dell' Università and INFN, Mostra D'Oltremare, 80125 Napoli, Italy

STUDY OF THE PROTON–AIR INELASTIC CROSS SECTION AT $\sqrt{S}$=1.6–2.4 TeV FROM EAS–TOP

INFN/AE–97/38
2 Luglio 1997

M.Aglietta[a,b], B.Alessandro[b], P.Antonioli[c], F.Arneodo[d,e], L.Bergamasco[b,f], M.Bertaina[b,f], C.Castagnoli[a,b], A.Castellina[a,b], A.Chiavassa[b,f], G.Cini Castagnoli[b,f], B.D'Ettorre Piazzoli[g], G.Di Sciascio[g], W.Fulgione[a,b], P.Galeotti[b,f], P.L.Ghia[b,f], M.Iacovacci[g], A.Lima de Godoi[h], G.Mannocchi[a,b], C.Morello[a,b], G.Navarra[b,f], O.Saavedra[b,f], G.C.Trinchero[a,b], P.Vallania[a,b], S.Vernetto[a,b],C.Vigorito[b,f].

a) Istituto di Cosmo-Geofisica del CNR, Torino, Italy
b) Istituto Nazionale di Fisica Nucleare, Torino, Italy
c) Istituto Nazionale di Fisica Nucleare, Bologna, Italy
d) Dipartimento di Fisica dell' Università dell'Aquila, L'Aquila, Italy
e) INFN Laboratori Nazionali del Gran Sasso, Assergi (AQ), Italy
f) Dipartimento di Fisica Generale dell' Università, Torino, Italy
g) Dipartimento di Scienze Fisiche dell' Università and INFN, Napoli, Italy
h)Instituto de Fisica Universidade de Sao Paulo, 01498-970 Sao Paulo, Brasil

ABSTRACT

The inelastic proton-air cross section is studied by means of the EAS-TOP Extensive Air Shower array (Campo Imperatore, 2005 m a.s.l., National Gran Sasso Laboratories), at $\sqrt{s} = 1.6 - 2.4$ TeV. Primary protons with fixed primary energy are selected from the muon size ($N_\mu(E_\mu > 1$ GeV)) and the shower size N_e ($N_e > N_e^0$). The p-air interaction mean free path is obtained from the frequency attenuation length in the atmosphere of showers with fixed electron number N_e. The closeness of the data to the Tevatron energies allows a direct comparison of $p - p$ and p-air cross sections.

INTRODUCTION

The $p - air$ inelastic cross section has been studied by cosmic-ray experiments through different techniques (Hara,1983, Baltrusaitis,1984, Akashi,1981 and Yodh,1972). The $p - p$ cross section has been accordingly derived by using $p - nucleus$ scattering models. In the present work we will use the EAS-TOP data to perform a measurement at proton energies $E_0 = (2 \div 4) \times 10^6$ GeV (corresponding to $\sqrt{s} \approx 2$ TeV) with the aim of obtaining a direct comparison with the Tevatron (Abe et al.,1994)(Ames et al.,1992) $p - p$ data, and to verify the commonly used scattering models for $p - nucleus$ collisions (Glauber and Matthiae,1970).

The method (Honda et al.,1983) is based on the selection of primary proton showers near to maximum development with fixed primary energy from the EAS muon size ($N_\mu^1 < N_\mu < N_\mu^2$), where $N_\mu = N_\mu(E_\mu > 1$ GeV)) and electron size ($N_e > N_e^0$). The $p - air$ interaction mean free path is obtained from the frequency attenuation length of such showers in the atmosphere, measured by selecting different observation zenith angles.

The response of the apparatus, the general method of the analysis, and the energy selection criteria have been established and verified by means of the CORSIKA code.

The data set is based on ≈ 10 million events , collected between 1993 and 1996, preliminary results are presented.

THE EXPERIMENT AND THE ANALYSIS

EAS-TOP is an Extensive Air Shower array located at Campo Imperatore (INFN National Gran Sasso Laboratories, 2000 m a.s.l., $x_0 = 810\,\mathrm{g/cm^2}$). The e.m. detector is made of 35 scintillator modules, 10 m^2 each, distributed over an area of $\approx 10^5 m^2$. For $N_e \geq 2.10^5$ the shower size, core location and arrival direction are measured with accuracy, respectively: $\frac{\sigma(N_e)}{N_e} \approx 10\%$, $\sigma_r \approx 5m$, and $\sigma_\theta \approx 0.5^0$ (Aglietta et al,1993).

The muon number N_μ is obtained by means of a tracking detector (140 m^2 area) made of 18 layers of streamer tubes and 9 layers of iron absorbers (13 cm thick). The readout is performed on orthogonal x and y views. A muon track is defined by the alignment of at least 6 hits in the tracking system; the energy threshold for vertical incidence is ≈ 1 GeV. The muon number is correctly derived up to $N_\mu \approx 30$ (Aglietta et al,1995,see also paper OG 6.1.6 at this conference).

In the following analysis, events with core distances between 50 and 150 m with respect to the muon detector are selected in order to avoid the saturation problems at small core distances and large primary energies, and small muon numbers at large core distances and low primary energies.

In order to select primary protons with fixed primary energy, the response of both the e.m. and muon detectors have been included in the CORSIKA code (Capdevielle,1992)(Knapp and Heck,1993); events are afterwards analyzed with the program codes used for the real data.

The procedure is made of the following steps:

- The detected muon number N_μ, for primary protons in the energy range above 2.10^6 GeV, core distance 50m $< r <$ 150m and zenith angle $\theta < 45^o$, has been fitted from the simulated data with the following expression

$\mathrm{N}_\mu = 1.87 \times 10^{-3} \times cos^2\theta \times E_0^{0.89} \times r^{-0.75} \times (1 + r/274.1)^{-2.5}$ (1)

- Events with primary energy in the interval $(2 \div 4)10^6$ GeV are selected using expression (1), given their core distance (r), zenith angle (θ) and detected muon number N_μ.

- A shower size threshold (N_e^0) is defined, from the simulation, at approximately the median of the corresponding distribution of the simulated shower sizes for vertical incidence. This corresponds to approximately 5% of the total rate of recorded events in the quoted energy range (slightly different cuts are performed in order to obtain an information on the systematics of the whole measurement), see tab 1.

- For the selected events ($N_\mu(E_1) < N_\mu < N_\mu(E_2)$, $N_e > N_e^0$) the frequency attenuation length in the atmosphere is calculated (taking into account the array acceptance at different zenith angles) for the simulated and physical events (for $1. < \sec\theta < 1.35$) fitting the expression

$$f(N_e, N_\mu, \theta) = f_0 \exp[-x_0(<\sec\theta> -1)/\lambda_{\mathrm{obs}}] \qquad (2)$$

- λ_{obs}^{sim} of the simulated data is compared to the interaction mean free path of the CORSIKA-HDPM model λ_{int}^{sim} to obtain the proportionality factor $k = \lambda_{obs}^{sim}/\lambda_{int}^{sim}$, with the assumption that this is essentially model independent and mostly representative of the shower fluctuations and the detectors' response (in fact the CORSIKA-HDPM model provides in general a good representation of the EAS-TOP data). The value of k in our energy region ranges from 1.4 for the smaller value of N_e^0 to ≈ 1 for large N_e^0 values.

- The frequency attenuation lengths in the atmosphere, calculated for the real data, are corrected with such values of k to obtain the experimental λ_{int} (see tab 1). - The contamination from He primaries, obtained from a simulation based on the same CORSIKA code, is included by assuming as a first approximation the same spectrum for p and He primaries at our energies, and λ_{int} is corrected with the corresponding value of λ_{He}. The final result of λ_{p-air} is also shown in tab 1, the quoted error includes a 30% uncertainty in the He flux.

Table 1: Results for different N_e^0 cuts in the energy range $(2 \div 4)10^6$ GeV of the various steps of the analysis. In the second row the fraction of selected events over the total number (vertical incidence) is shown. $\lambda_{\rm obs}$ is derived directly from the experimental data, $\lambda_{\rm int}$ is the value after the correction over the factor k (from the simulation) and $\lambda_{\rm p-air}$ is the final value obtained after the correction over the He contamination.

$LogN_e^0$	6.0	6.1	6.2	6.3	6.4
sel. ev.(%)	8.6	4.3	1.9	0.8	0.4
$\lambda_{\rm obs}({\rm g/cm^2})$	79.7 ± 1.1	77.0 ± 1.5	73.0 ± 2.1	80.5 ± 3.6	78.7 ± 5.2
k	1.41 ± 0.06	1.18 ± 0.06	1.18 ± 0.08	1.11 ± 0.16	1.09 ± 0.30
$\lambda_{\rm int}({\rm g/cm^2})$	56.3 ± 2.4	65.1 ± 3.5	61.7 ± 4.7	72.1 ± 10.8	71.9 ± 20.5
He (%)	37	34	23	0	0
$\lambda_{\rm p-air}({\rm g/cm^2})$	66.2 ± 4.0	78.3 ± 5.4	68.3 ± 6.1	72.1 ± 10.8	71.9 ± 20.5

RESULTS AND DISCUSSION

As we can see from tab. 1 the different N_e^0 cuts, in spite of the different selection criteria, provide consistent results on λ_{p-air} (for large N_e^0, errors can be reduced by improving the statistic of the simulation).

By averaging all of them we obtain:

$$\lambda_{p-air} = 70.1 \pm 2.5 {\rm g/cm^2}$$

and from $\sigma_{\rm in}^{p-\rm air} = 2.41 \times 10^4/\lambda_{p-air}$

$$\sigma_{\rm in}^{p-\rm air} = 343.8 \pm 12.3mb$$

This value is slightly lower than the average behaviour of the fit of accelerators and EAS data (Honda et al.,1993)

Comparing this value with the Tevatron total cross section measurements ($\sigma_{\rm tot}^{\rm pp} = 72.8 \pm 3.1$mb, $\sigma_{\rm tot}^{\rm pp} = 80.03 \pm 2.24$mb), it results that it is smaller than expected by some $p - nucleus$ scattering models as e.g. Durand-Pi (Durand and Pi,1988), while it is in better agreement with other theoretical predictions (Bellandi et al.,1995)(Gaisser,1987). It is also well consistent with the value used in CORSIKA-HDPM code.

REFERENCES

T.Hara et al, Phys. Rev. Lett., 50,2058,(1983).
M.Akashi et al.,Phys. Rev. D,24,2353,(1981).
Yodh et al, Phys. Rev. Lett.,28,1005,(1972).
K.M.Baltrusaitis et al., Phys. Rev. Lett.,52,1380,(1984).
CDF Coll. F. Abe et al., Phys. Rav D, 50,5550,(1994).
E710 Coll. N.A. Ames et al. Phys. Rev. Lett., 68,2433,(1992).
R.J. Glauber and G. Matthiae, Nucl. Phys,B21,135,(1970).
J.N. Capdevielle et al, Report KfK 4998,(1992).
J. Knapp and D. Heck, Report KfK 5196B,(1993).
M. Aglietta et al., Nucl. Instr. and Meth. in Phys. Res.,A336,310,(1993).
M. Aglietta et al., Proc. 24th ICRC, Rome, vol 2,664,(1995).
L. Durand and H.Pi, Phys. Rev. D,38,78,(1988).
M.Honda et al, Phys. Rev. Lett., 70,525,(1993).
J. Bellandi et al., Phys. Lett.,343B,410,(1995).
T.K. Gaisser et al, Phys. Rev. D,36,1350,(1987).

THE HADRON SPECTRUM AT 840 gcm^{-2} AVERAGE ATMOSPHERIC DEPTH

INFN/AE–97/39
2 Luglio 1997

M.Aglietta[a,b], B.Alessandro[b], P.Antonioli[c], F.Arneodo[d,e], L.Bergamasco[b,f], M.Bertaina[b,f], C.Castagnoli[a,b], A.Castellina[a,b], A.Chiavassa[b,f], G.Cini Castagnoli[b,f], B.D'Ettorre Piazzoli[g], G.Di Sciascio[g], W.Fulgione[a,b], P.Galeotti[b,f], P.L.Ghia[b,f], M.Iacovacci[g], G.Mannocchi[a,b], C.Morello[a,b], G.Navarra[b,f], H.Nogima[h],O.Saavedra[b,f], G.C.Trinchero[a,b], P.Vallania[a,b], S.Vernetto[a,b],C.Vigorito[b,f].

a) Istituto di Cosmo-Geofisica del CNR, Torino, Italy
b) Istituto Nazionale di Fisica Nucleare, Torino, Italy
c) Istituto Nazionale di Fisica Nucleare, Bologna, Italy
d) Dipartimento di Fisica dell' Università dell'Aquila, L'Aquila, Italy
e) INFN Laboratori Nazionali del Gran Sasso, Assergi (AQ), Italy
f) Dipartimento di Fisica Generale dell' Università, Torino, Italy
g) Dipartimento di Scienze Fisiche dell' Università and INFN, Napoli, Italy
h) Instituto de Fisica, Universidade Estadual de Campinas, Campinas–SP, Brasil

ABSTRACT

The all–hadron flux is measured at the average atmospheric depth of 840 gcm^{-2} in the energy range 50 GeV–10 TeV by means of the hadron calorimeter of EAS-TOP. The operation and resolution of the detector are described; the measured vertical flux is $S(E_h)\ dE_h = (1.89 \pm 0.21) \times 10^{-7}\ (E/1TeV)^{-(2.69 \pm 0.14)}$ m^{-2}s^{-1}sr^{-1}GeV^{-1}, in good agreement with the results of other experiments when converting to different atmospheric depths.

INTRODUCTION

The EAS–TOP Extensive Air Shower array is located at Campo Imperatore (2000 m a.s.l.) above the underground Gran Sasso Laboratories (Aglietta et al.,1993). Its aim is to perform multicomponent EAS observations, i.e. study the electromagnetic, muonic (at $E \geq 1$ GeV, and at $E \geq 1$ TeV in correlation with undeground detectors), Cherenkov and hadronic components. The hadron detector is running in correlation with the EAS array (EAS–TOP Collaboration, 1997) and as a standalone apparatus; its main aims are the study of the hadron flux, uncorrelated and in EAS, and the absorption characteristics of the EAS cores. Its data, correlated to EAS ones and to measurements at different atmospheric depths, provide informations on the hadronic absorption length and the cosmic ray primary composition.

THE DETECTOR

The EAS–TOP calorimeter MHD (Muon and Hadron Detector) is a 140 m^2, 814 g cm^{-2} thick detector; it consists of nine identical planes, each made of one layer of quasi proportional tubes for hadron calorimetry, 2 layers of streamer tubes for particle tracking and a 13 cm thick iron absorber, for a total depth of $\simeq 6.2$ nuclear mean free paths. The tubes, 12 m long and (3×3) cm^2 section, are operated with an Argon–Isobutane 50/50 gas mixture distributed in parallel over the 23 tubes of each half–plane. Between the 7th and 8th layer, a set of six (80×80) cm^2 scintillators, identical to those used in the EAS–TOP electromagnetic detector is lodged for triggering purposes. The proportional tubes are operated in saturated proportional mode at a voltage of 2900 V; the induced charge is picked up by 840 (40×38) cm^2 pads, covering a total area of 128 m^2. On average, the ADC dynamic is saturated at about 1200 particles/pad.

The in–situ response of the detector is periodically checked in devoted calibration runs. The mean charge induced on each pad by single minimum ionizing particles and the pad inefficiency are measured by using a single muon trigger; the average induced charge/pad for a single particle is $\simeq$ 0.82 pC. The detector stability is continuously monitored, checking for temperature, pressure and gas mixture variations.

In order to study the detector response to different particle densities and check the results of a simulation including the modelling of the tube response, a prototype apparatus has been tested at a 50 GeV positron beam at the CERN–SPS accelerator at CERN. It included the same chambers with similar gas mixture as the MHD ones, but with reduced length (1.2 m), seen by three pads; the power supply was fixed at 3200 V, to reproduce at sea level the same signals as at the site of the experiment. The target was given by a layer of 4 cm lead, the air gap between the first pad and the absorber was 5 cm.

The results of the test beam measurements are shown in Fig.1 (white triangles): a) the response to different primary energies from 2 to 50 GeV: a small saturation effect is seen at energies $\geq$ 30 GeV; b) the measured longitudinal development of the cascade in iron.

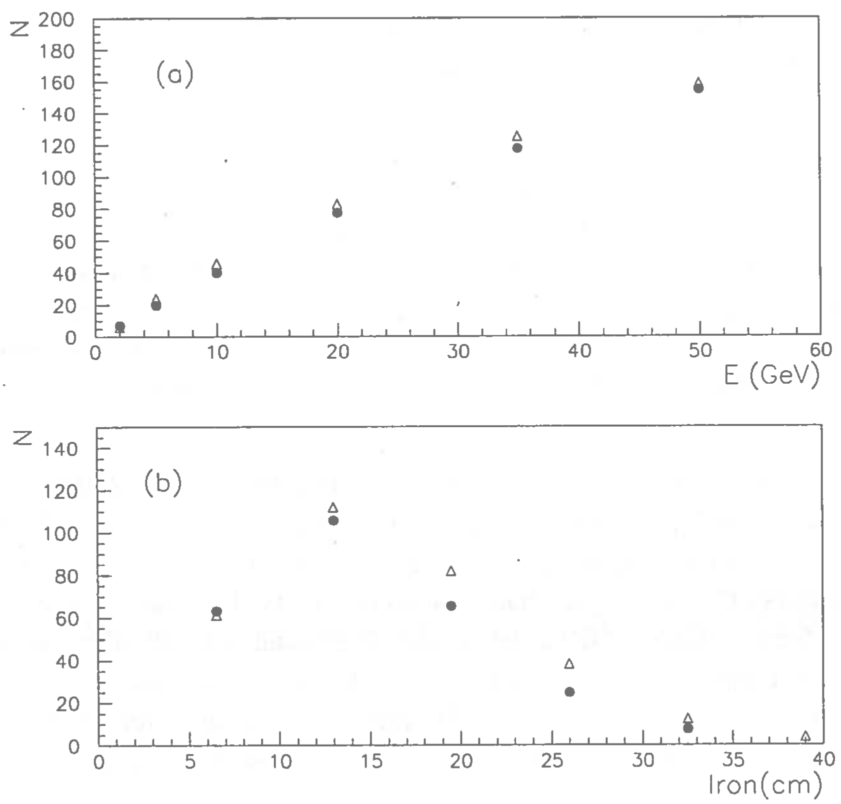

Fig. 1: Comparison between the test beam measurements (white triangles) and the Monte Carlo simulation (black circles) (a,b: see text).

The response of the calorimeter to hadronic showers has been studied by means of a full Monte Carlo simulation based on the Geant code (R.Brun et al.,1984); the Fluka option has been chosen to model the hadronic interaction. The detector behaviour in quasi proportional mode has been modelled in terms of the ionization density produced by charged particles. The saturation in the collected charge is relevant for tracks crossing the tube at angles $\theta \leq 15^0$; its detailed study has been used to introduce the density saturation effect. Fluctuations in the ionization energy losses inside the proportional tubes and in the charge induced by individual particles and in showers have been included, together with a 16% systematic fluctuation. The comparison between the experimental data and the simulated response to electromagnetic showers is shown in Fig.1 (black circles); the difference between the two sets of data is less than a few percent. Furthermore, an excellent agreement was found in the measurement of the induced charge without air gap between the pad and the absorber, thus confirming the goodness of the model describing the behaviour of the detector at the highest particle densities. The same particle density obtained at 50 GeV after 4 cm of lead is found for iron absorber and the MHD geometry at about 650 GeV, which is therefore the effective calibration upper energy.

DATA ANALYSIS

The trigger condition to select single hadrons in the calorimeter is given by the analogical OR of the six scintillator on top of the 7th plane. A total of 589385 events were selected in 408 days. An event is accepted as a hadron if the maximum energy deposit in at least three planes (including the 7th one) is found on the same pad over an area $A_1 = (3 \times 3)$ pads centered on the triggering scintillator. With such a configuration, "quasi vertical" events ($< \theta >= 15.4^0$) are selected; the efficiency for getting events at $\theta \geq 30^0$ is below 50%. The trigger efficiency reaches 80% for $E \approx 100 \ GeV$. The total number of particles is found summing up the signals induced on an area $A_0 = (7 \times 7)$ pads on all the nine layers of the calorimeter.

In order to convert the total number of "induced particles" to the hadron energy, a complete set of simulations has been run requiring the same trigger configuration, for fixed primary energies. The conversion curve from the total number of particles induced on the pads to the primary energy is given in Fig.2; non linear effects are taken into account and corrected for. The calorimeter resolution for single hadrons is shown in Fig.3; the 15% resolution at 1 TeV deteriorates to $\simeq$ 25% at 5 TeV (due to leakage losses) and to $\simeq$ 40% at 30 GeV (due to sampling losses).

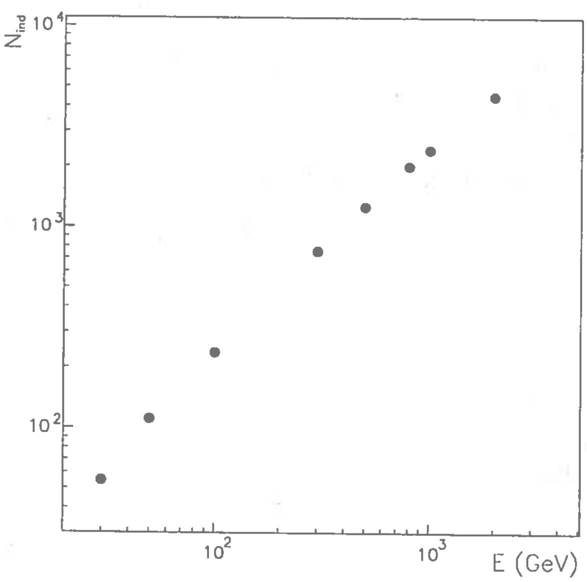

Fig. 2: Total number of induced particles versus the primary energy.

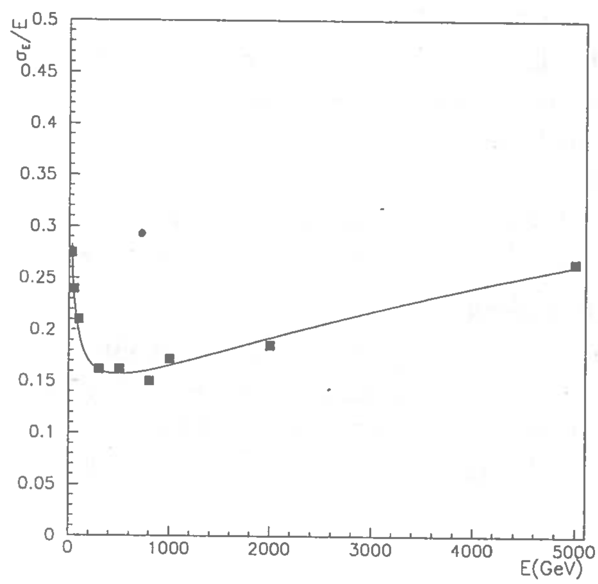

Fig. 3: Energy resolution. Full line: best fit to the simulated points.

A preliminary analysis was performed on a reduced sample of data, referring to one of the six triggering scintillators. Using the calibration curve of Fig.2 and the effective area $A_{eff}(\theta, E)$ as calculated using the simulated data, we obtain the all–hadron flux at the average depth of $840 = 810/cos(< \theta >)$ g cm^2) shown in Fig.4. No correction for systematic uncertainties and trigger inefficiencies is introduced in these data.

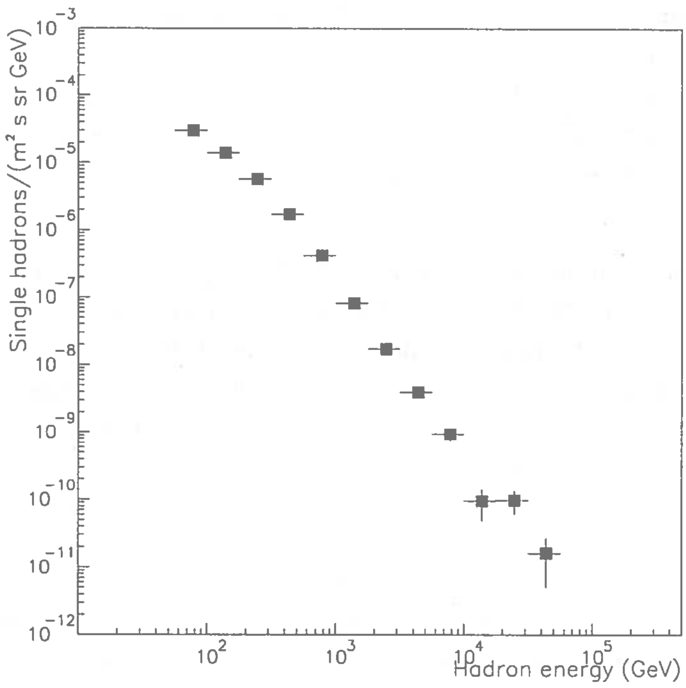

Fig. 4: Hadron energy spectrum at $840 g\ cm^{-2}$.

CONCLUSION

The EAS–TOP calorimeter is currently operating as a high stability hadron detector. Preliminary data on the hadron flux at the average atmospheric depth of 840 g cm^{-2} are obtained. Around 1 TeV, they can be fitted with the expression $S(E_h)\ dE_h = (1.89 \pm 0.21) \times 10^{-7}\ (E/TeV)^{-(2.69\pm0.14)}$ m^{-2}s^{-1}sr^{-1}GeV^{-1}. These data are in good agreement with the results of the Kascade Collaboration (Mielke H.H. et al., 1994) if an attenuation length of $\Lambda \approx 120$ g cm^{-2} is used to extrapolate the flux to the sea level.

REFERENCES

M.Aglietta et al., *Nucl.Instr.Meth.*, **A336**, 310 (1993).
EAS–TOP Collaboration, *this Proceedings*, OG 6.2.4 (1997).
R. Brun et al., *CERN report*, DD/EE/84–1 (1984).
H.H.Mielke et al.,*J.Phys.G: Nucl.Part.Phys.*, **20**, 637 (1994).

PRIMARY COMPOSITION ANALYSIS FROM MUONS IN EAS

INFN/AE–97/40
2 Luglio 1997

ABSTRACT

The cosmic ray composition is studied in the energy range around the knee ($E_0 \approx 3 \cdot 10^{15} eV$) of the primary energy spectrum with the Extensive Air Shower (EAS) detector of the EAS-TOP experiment at the National Gran Sasso Laboratories. The experimental data are compared with the expectations from a simulation based on the Dual Parton Model (CORSIKA code) and a cosmic ray composition extrapolated from low energy direct measurements. The average values of the measured muon lateral distribution function ($E_\mu > 1\ GeV$), the $N_e - N_\mu$ relation and the fluctuations of muon numbers are well reproduced by the simulation. The same interaction model with mixed composition, and the Peters-Zatsepin hypothesis on the rigidity dependence of the knee, reproduce correctly the data also above the knee.

INTRODUCTION

The primary composition is studied through the EAS electron and muon components recorded by the EAS-TOP array. First analysis were presented at the Rome Conference (EAS-TOP collab., 1995) in the energy region below the knee. In this paper we extend the previous results to the region just above the knee.

The EAS-TOP array is located at Campo Imperatore (2005 m a.s.l., 810 g/cm^2 atmospheric depth), above the underground Gran Sasso Laboratories. The electromagnetic (e.m.) detector consists of 35 modules of plastic scintillators (10 m^2 each, 4 cm thick), distributed over an area of $\approx 10^5 m^2$ (Aglietta et al., 1993). The resolutions in measuring the core location (X_c, Y_c) and the shower size N_e are in the energy range of our analysis ($N_e > 10^{5.3}$) $\sigma_{\Delta X_c} = \sigma_{\Delta Y_c} \approx 5\,m$ and $\sigma_{N_e}/N_e \approx 0.1$. The EAS arrival directions are measured from the times of flight among the different modules with accurancy $\delta\theta = 0.5°$. The muon detector (Aglietta et al., 1991) is a tracking module consisting of 9 active planes, 30 cm away from each other, interleaved with iron absorbers 13 cm thick for a total height of about 280 cm. Each plane includes two layers of streamer tubes for muon tracking, the total surface of the detector is $A \sim 12 \times 12\,m^2$. The X coordinate of muon track is obtained from the signals of the anode wires (368 in a layer), the Y coordinate from the induced signals on strips orthogonal to the wires. The distance among the wires and the width of the strips is 3 cm. The Z coordinate is given by the height of the layer with respect to the ground. A muon track is defined from the alignment of at least 6 hits (wires on) in different layers of tubes. The muon energy threshold for vertical events is 1 GeV.

THE DATA AND THE SIMULATION

In the following analysis we select a sample of experimental events for which the shower core is inside the edges of the e.m. array (internal events), the zenithal angle $\theta < 17.7°$, and $N_e > 10^{5.3}$. The last requirement to restrict the analysis around the knee where $Ne_{knee} \approx 10^{6.07}$ corresponds at a primary energy $E_{knee} \approx 2.8 \cdot 10^{15} eV$ for primary protons. For each event we measure the EAS size N_e, the arrival direction (θ and ϕ) and the core location X_c, Y_c to get the distance R between the EAS core and the muon detector. The number of muons detected by the tracking system in the X-Z plane (N_μ^x) is used to obtain the muon density (ρ_μ) and hence the total muon number (N_μ) in the shower. The subtraction of accidental muons and the acceptance of the detector are taken into account when calculating N_μ.

The CORSIKA code (Capdevielle et al., 1992) and a mixed composition model extrapolated from direct measurements (JACEE Coll., 1993, and CRN Coll., 1991) are used to simulate the events according to tab.1. The interactions of the muons crossing the tracking detector and its response are simulated using the GEANT code (Brun et al., 1984). Simulated events are analysed with the same programs used for the real ones.

RESULTS AND DISCUSSION

The average muon density is calculated binning the events in intervals of size and R to obtain an average muon lateral distribution. In fig.1 the lateral distributions in the regions just below ($10^{5.8} < N_e < 10^{6.0}$), and above the knee ($10^{6.0} < N_e < 10^{7.0}$) are shown. The average muon lateral distribution function is well fitted by the Greisen formula (Greisen K., 1960):

$\rho_\mu(R) = C \cdot R^{-0.75}(1 + R/R_\circ)^{-2.5}$ where $\rho_\mu(R)$ is the muon density at distance R, C is a normalization factor and $R_\circ = 400\ m$ gives the slope of the lateral distribution. This function is used to obtain N_μ. In fig.1 the experimental data are compared with pure proton, helium and iron compositions and the mixed one. Two composition models are adopted above the knee : the Peters-Zatsepin (P-Z) hypothesis ($E_{knee}(Z) = Z \cdot E_{knee}(proton)$) (Peters, 1959, and Zatsepin, 1962), and a constant energy knee $E_{knee}(Z) = E_{knee}(proton)$. The difference $\Delta\gamma$ between the values of the spectral index (γ) below and above the knee is the same for each element of the composition ($\Delta\gamma = 0.5$).

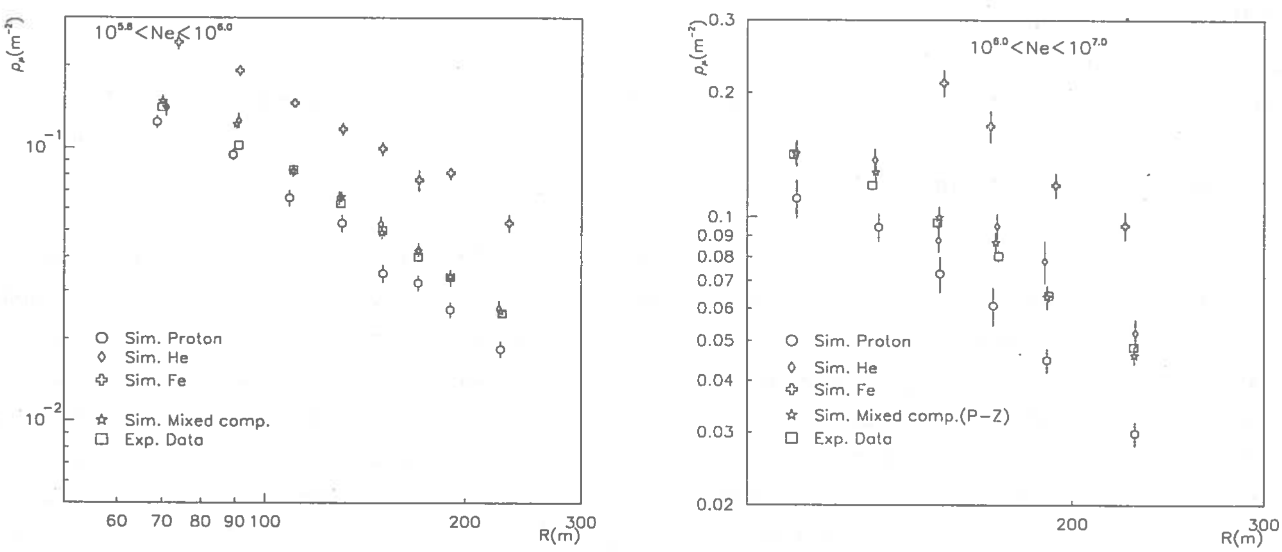

Fig. 1: Muon lateral distribution

The mean values of N_μ in intervals of N_e is shown for experimental and simulated events in fig.2. The point above the knee is given for both models. The agreement is better than $\approx$ 10%, and the changes in composition around the knee have to be smooth as we can see from fig.3 in which the ratio of the experimental to the simulated average muon numbers $< N\mu >$ is plotted vs Ne for the two mixed compositions.

The fluctuations of the muon numbers are analysed, in the range $10^{5.8} < N_e < 10^{6.0}$ and $10^{6.0} < N_e < 10^{7.0}$ in the interval $80\ m < R < 160\ m$, by calculating for each event the ratio $N_\mu / < N_\mu >$ in which $< N_\mu >$ is given by the expression $< N_\mu > = 1.315 \cdot N_e^{0.744}$ obtained by fitting the $< N_\mu > - N_e$ relation of the experimental data. In fig.4 the distribution of such ratio is plotted for the mixed composition and experimental data below the knee. The mixed composition shows a good agreement with the data also in the region of larger fluctuations, dominated by proton and iron primaries as shown in fig.5 in which the contribution of each element is plotted. The same conclusions hold in the region above the knee (figs.6 and 7). In a paper presented in this conference, it is shown that the measured and simulated extreme fluctuations are the ones expected for proton-like and iron-like primaries. These primaries are selected on the basis of the correlated EAS-TOP (N_e) and LVD (N_μ^{TeV} and $\Delta E_\mu / \Delta L$) data (see these proceedings HE 2.1.8).

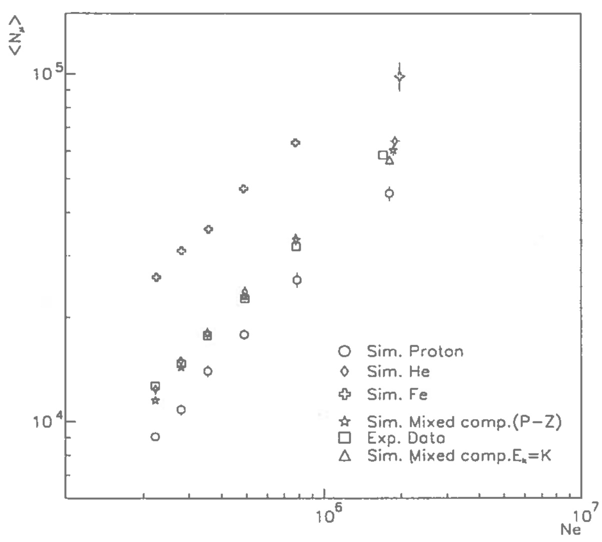

Fig. 2: $< N_\mu > vs N_e$

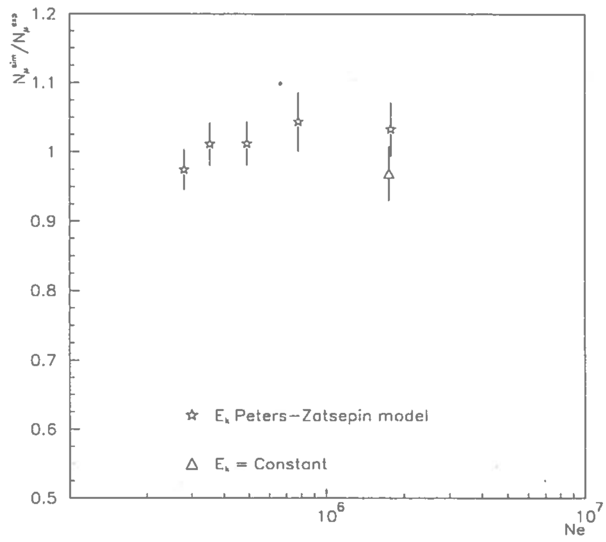

Fig. 3: $< N\mu >_{mix.} / < N\mu >_{exp.}$ *vs Ne*

We can thus conclude that the mixed composition defined above, and the Dual Parton Model of high energy hadronic interactions (CORSIKA code) reproduce the experimental data concerning the average muon lateral distributions, the $N_e - N_\mu$ relation and muon fluctutations both in the region below and above the knee. This last region is better described by the Peters-Zatsepin prediction, although a constant composition cannot be excluded within the present statistics (see fig.3). The analysis of muon production heights is in progress.

	γ	$F(>1TeV)$ $m^{-2}\ s^{-1}\ sr^{-1}$	$E_{knee}^{P.-Z.}(TeV)$
p	2.75	$19.7 \cdot 10^3$	$2.84 \cdot 10^3$
He	2.65	$5.64 \cdot 10^3$	$5.67 \cdot 10^3$
N	2.65	$1.55 \cdot 10^3$	$1.98 \cdot 10^4$
Mg	2.65	$0.71 \cdot 10^3$	$3.40 \cdot 10^4$
Fe	2.65	$1.97 \cdot 10^3$	$7.37 \cdot 10^4$

Table 1: *Mixed composition model parameters*

REFERENCES

EAS–TOP collaboration, *Proc. 24rd ICRC*, Rome, 2, 664 (1995).
M. Aglietta et al., *Nucl.Instr.Meth.Phys. Res.*, A 336, 310 (1993).
M. Aglietta et al., *Proc. 22rd ICRC*, Dublin, HE 3.6.31, (1991).
R. Brun et al., CERN report DD/EE/84–1 (1984).
J.N. Capdevielle et al., *The Karlsruhe EAS Simulation Code CORSIKA*, KfK Report 4998, (1992).
CRN collaboration, *Ap. J.*, 374, 356 (1991)
K. Greisen, *Ann.Rev.Nuclear Science*, 10, 78, (1960).
JACEE collaboration, *Proc. 23rd ICRC*, Calgary, 2, 25 (1993).
B. Peters, *Proc. 6th ICRC*, Moscow, 3, 157 (1959).
G.T. Zatsepin et al., Izv. Ak. Nauk USSR, SP, 26, 685 (1962).

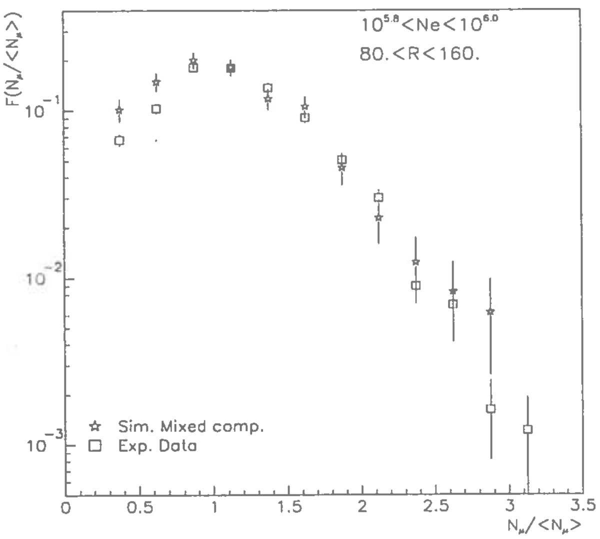

Fig. 4: Muon number fluctuations

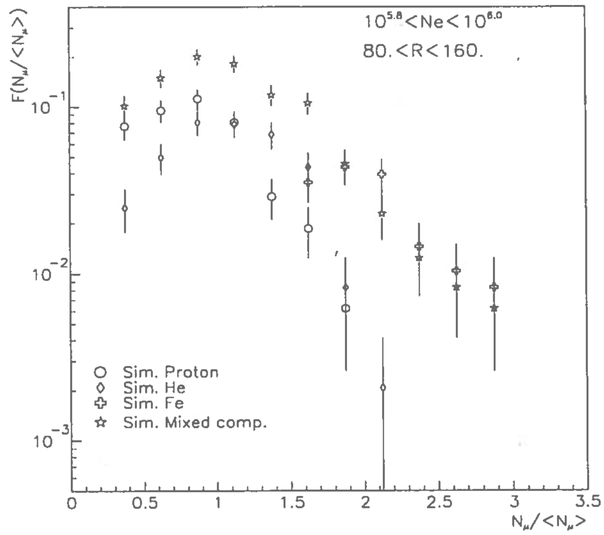

Fig. 5: Contribution of each element in the muon number fluctuations

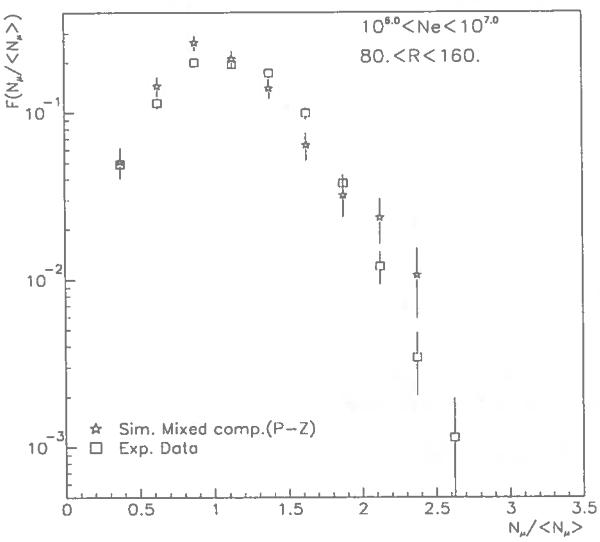

Fig. 6: Muon number fluctuations

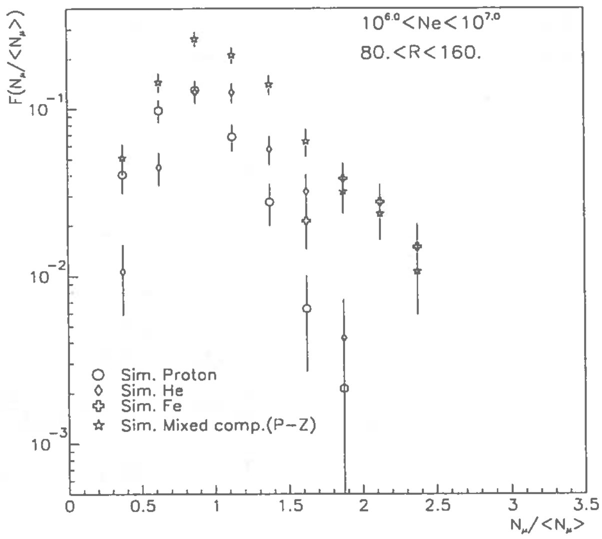

Fig. 7: Contribution of each element in the muon number fluctuations

STUDY OF THE EAS CORES IN THE KNEE REGION

INFN/AE–97/41
2 Luglio 1997

M.Aglietta[a,b], B.Alessandro[b], P.Antonioli[c], F.Arneodo[d,e], L.Bergamasco[b,f], M.Bertaina[b,f], A.Campos Fauth[g], C.Castagnoli[a,b], A.Castellina[a,b], A.Chiavassa[b,f], G.Cini Castagnoli[b,f], B.D'Ettorre Piazzoli[h], G.Di Sciascio[h], W.Fulgione[a,b], P.Galeotti[b,f], P.L.Ghia[b,f], M.Iacovacci[h], G.Mannocchi[a,b], C.Morello[a,b], G.Navarra[b,f], H.Nogima[g], L.Riccati[b], O.Saavedra[b,f], G.C.Trinchero[a,b], P.Vallania[a,b],S.Vernetto[a,b], C.Vigorito[b,f]

a) Istituto di Cosmo-Geofisica del CNR, Corso Fiume 4, 10133 Torino, Italy
b) Istituto Nazionale di Fisica Nucleare, Via Pietro Giuria 1, 10125 Torino, Italy
c) Istituto Nazionale di Fisica Nucleare, Via Irnerio 46, 40126 Bologna, Italy
d) Dipartimento di Fisica dell' Università dell'Aquila, Via Vetoio, 67010 L'Aquila, Italy
e) INFN Laboratori Nazionali del Gran Sasso, S.S. 17 bis, 67010 Assergi (AQ), Italy
f) Dipartimento di Fisica Generale dell' Università, Via P. Giuria, 1, 10125 Torino, Italy
g) Instituto di Fisica, Universidade Estadual, Barao Geraldo, 13081 Campinas (SP), Brazil
h) Dipartimento di Scienze Fisiche dell' Università and INFN, Mostra D'Oltremare, 80125 Napoli, Italy

ABSTRACT

A study of the EAS cores is performed with the hadron calorimeter of the EAS-TOP array (INFN National Gran Sasso Laboratories), at primary energies $E_0 \geq 100$ TeV, concerning the total energy content, and absorption characteristics of EAS in the core region. The same study is performed for the identified multicore events.

INTRODUCTION

The study of the properties of EAS cores is of interest both for the study of the primary composition at EAS energies, and of some features of hadron interaction at high energies(mainly large P_T from multicore events and energy content of the hadron and e.m. EAS components). We present in this note some phenomenological results obtained with the EAS-TOP calorimeter at primary energies $E_0 \approx 10^{15} eV$.

THE EAS-TOP EXPERIMENT

The EAS-TOP experiment is located at Campo Imperatore (2010 m a.s.l., atmospheric depth $x_0 = 810 g\ cm^{-2}$), and includes different detectors of the EAS components. We are interested here in the electromagnetic (EMD) and a hadron detector (MHD) data (Aglietta et al.,1993).

- EMD consists of 35 modules of scintillator, 10 m^2 each, spread over an area of $\approx 10^5$ m^2. From the sample of the particle densities at the different sites and the time of flight technique, the core location, the slope of the $l.d.f.$, the shower size and the arrival direction are obtained. For $N_e \geq 2.10^5$ the shower size, core location and arrival direction are measured with accuracy, respectively: $\frac{\sigma(N_e)}{N_e} \approx 10\%$, $\sigma_r \approx 5m$, and $\sigma_\theta \approx 0.5^0$.

- MHD consists of 9 levels of 13 cm thick iron absorbers for an equivalent thickness of 820 $gr\ cm^{-2}$. Each level contains two layers of streamer tubes for muon tracking and one layer of "quasi" proportional tubes for hadron calorimetry. At the moment the uppermost level (9^{th}) is unshielded and used to detect the e.m. component of EAS. The read-out of each layer is done through the induced signals on 840 pads (0.16 m^2 each, organized in a 28 × 30 matrix) covering a total area of 128 m^2 . The charge response of each pad is periodically checked and measured using cosmic-rays muons and corrected for the pressure and temperature variations during data taking. Finally 8 (.8 × .8m^2) scintillators counters, identical to those of the EAS-TOP e.m. detector are located above the 9^{th} plane: 4, internal $S_{i,int}$, are placed at about 3 m from the calorimeter center and 4, external $S_{i,ext}$, outside the MHD structure at the corners position. They are used to select contained EAS cores.

DATA SELECTION

A selection of EAS events with the core inside a fiducial area of $8 \times 8m^2$ internal to the 9^{th} level of the detector is performed asking for the following conditions.

- At least 2000 particles on the uppermost (9^{th}) level of the detector.
- Ratio $R = \frac{\sum_{i=1,4} S_{i,ext}}{\sum_{i=1,4} S_{i,int}}$ of the total number of particles seen by external and internal scintillator < 1.
- Arrival direction determined by means of the EMD data.
- Final fitted position of the core through the pad particle densities internal to the fiducial area.

The size(Ne) and slope(s) of the l.d.f. of the shower are obtained through the best fit (running MINUIT standard routines) of the particle density distribution to the NKG formula $\rho(r) = \frac{Ne}{(r_0)^2}(1+\frac{r}{r_0})^{s-4.5}(\frac{r}{r_0})^{s-2}$ using as sample points both MHD($9^{th} layer$) and EMD data. All experimental fluctuations for EMD modules and MHD pads are taken into account during the minimization process. In fig.1 the size spectrum of the selected events is shown, compared to the EAS-TOP size spectrum (EAS-TOP Collaboration, O.G. 6.2.4, 1997).

THE CORE ENERGY CONTENT

The study of the core region, as a first approach, is achieved by investigating the electromagnetic, hadronic and full energy content of the shower core inside cylinders of 2.4 m at different absorption layers, precisely: layer 8 (P8), that is ≈ 0.78 nuclear interaction lengths (λ), for the e.m. energy, layer 4 (P4) ($\approx 3.88\lambda$) for the hadronic one, and the sum of the 8 shielded layers (Σ P) ($\approx 6.20\lambda$) for the total energy.

The distributions of the number of particles detected in these cylinders are compared with the size spectrum, obtained from the e.m. detector, shown in fig. 1 (EAS-TOP Collaboration, O.G. 6.2.4, 1997). The comparison is made imposing that multiplying the density distributions (d) for these coefficients (k), the number of events at $(d \cdot k) > 10^{5.5}$ is the same of the N_e distribution of the selected events. The graphs are shown in figs. 2-4 compared to the size spectrum fit also shown in fig. 1.

From figs. 2-4 it appears that the distributions are quite similar, and that the energetic content of the core in the different components, at this very first stage, looks quite constant in the considered energy range.

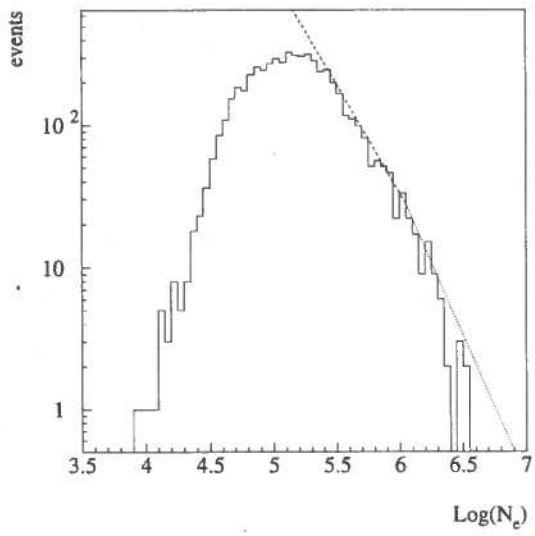

Fig. 1: Size distribution of the selected events compared with the Ne spectrum obtained by the electromagnetic detector.

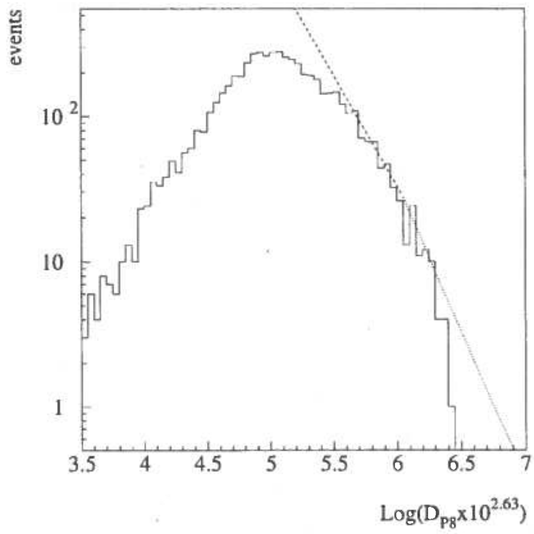

Fig. 2: Distribution of the particle density of the 8^{th} *layer (mainly due to the e.m. energy release) in a 2.4 m cylinder.*

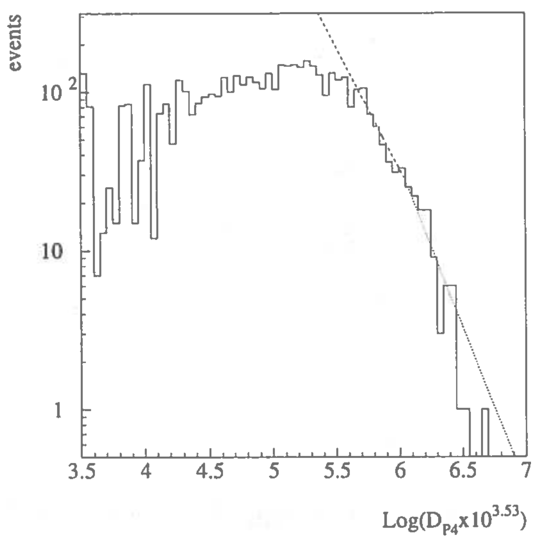

Fig. 3: Same as fig.2, but for layer 4 where only hadronic energy release is expected.

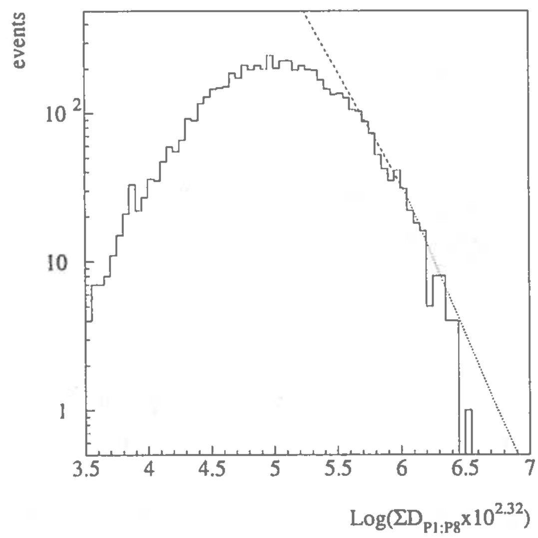

Fig. 4: Same as fig.2, but for the sum of the 8 shielded layers(e.m. and hadronic components).

THE MULTICORE EVENTS

Multicore events were detected in EAS, and interpreted as due to large P_T jet production in the energy region $\sqrt{s} \approx 500GeV$ (Chudakov A.E. et al.1983, Aglietta et al.,1995, Aglietta et al. 1996). We present here the preliminary results of a systematic "quasi" automatic selection of a set of multicore events by means of the evaluation of the total subcore significance after subtracting the contribution from the main shower. The confidence level is established by means of a simulation taking into the account all experimental fluctuations. The shower size is in the range $10^{4.8} \leq Ne \leq 10^{5.8}$, i.e. $E_0 \approx 500TeV$, $\sqrt{(s)} \approx 1TeV$ in the center of mass.

The subcore energy (E_{sub}) and production height (h_{max}) are obtained in the e.m. approximation, i.e.: $E_{sub} \propto \frac{r_M \cdot n}{R} GeV$, $h_{max} = h(E_{sub}, s = 1)$, where r_M is the Moliere radius and n the number of particles recorded by the pads identifying the subcore inside a distance $\leq R$. Therefore through the relation $P_T = \frac{E_{sub} \cdot r}{h_{max}}$ the associated transverse momentum is obtained, where r is the distance between the cores. The values obtained range from 10 to 40 TeV with an average value $E_{sub} \approx 23.2\, TeV$. A distribution of the calculated transverse momenta for the must significant selected events is shown in fig. 5. The measurement of the total energy release in the MHD detector has been obtained by integrating the total number of particles in a cylinder (radius 1 m) centered on the core and subcore positions and following the shower direction. The conversion formula from the number of particles to the energy release is obtained through a full simulation of the detector response (EAS-TOP Collaboration, H.E. 1.2.23,1997). The averaged value of energy release is $E_{rel} \approx 1.1\, TeV$. The expected energy release in the calorimeter for primary proton showers is $E_{rel} \simeq \frac{E_p}{(40 \div 50)}$. For the subcore such value is $E_{rel} \simeq \frac{E_{sub}}{20}$. Such difference agrees with the hypothesis that the subcore are selected near their maximum development. Further an indication of the contribution of the e.m. and hadronic content of the subcore can be obtained from the energy release at different absorber levels. The ratios ($\frac{\rho_5}{\rho_8}$) between the particle densities recorded at the 5^{th} (409 g cm^{-2}) and the 8^{th} (102 g cm^{-2}) layer around the main and subcores are shown in figs. 6 and 7.

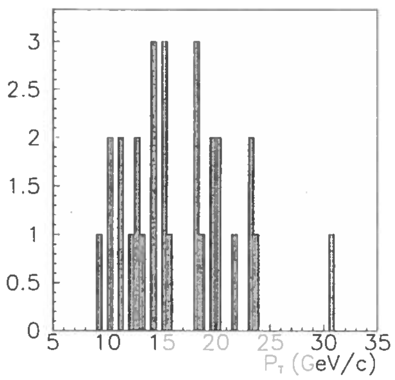

Fig. 5: P_T Distribution for the subcores

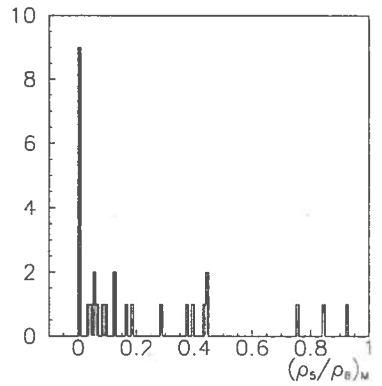

Fig. 6: The ratio ($\frac{\rho_5}{\rho_8}$)$_M$ for the main core

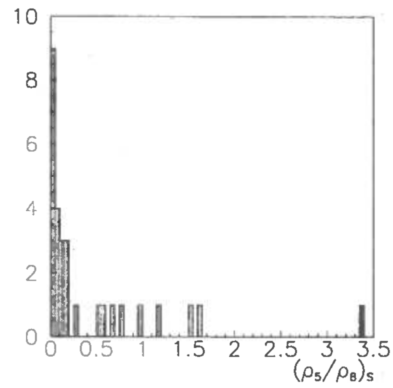

Fig. 7: The ratio ($\frac{\rho_5}{\rho_8}$)$_S$ for the sub core

The averaged values are respectively ($\frac{\rho_5}{\rho_8}$)$_M = 0.21 \pm .26$ for the main- core and ($\frac{\rho_5}{\rho_8}$)$_S = 0.45 \pm .71$ for the sub-core, and this confirms an higher hadronic content of the subcores with respect to the main shower core.

CONCLUSIONS

Phenomenological data from the EAS-TOP calorimeter are presented. Detailed simulations are in progress for a systematic interpretation of the measurements. The statistics is being improved to obtain a reasonable number of events above the knee of primary spectrum.

REFERENCES

Aglietta, M. et al., EAS–TOP Collaboration, *Nucl. Instr. and Meth.*, **A336**, 310 (1993).

Aglietta, M. et al., EAS–TOP Collaboration, *Proc. 24rd ICRC,* Rome, **2**, 293 (1995).

EAS-TOP Collaboration, *These Proceedings*, O.G. 6.2.4 (1997).

EAS-TOP Collaboration, *These Proceedings*, H.E. 1.2.23 (1997).

Aglietta, M. et al., EAS–TOP Collaboration, *Topics in cosmogeophysics* Bologna, 58 (1996).

Chudakov A.E. et al., *Proc. 17th ICRC,* Paris, **6**, 183 (1981).

STUDY OF THE KNEE OF THE COSMIC RAY SPECTRUM IN THE ELECTRON COMPONENT

INFN/AE–97/42
2 Luglio 1997

ABSTRACT

The shape of the EAS size spectrum around the knee is discussed following the EAS–TOP electromagnetic detector data. The shower size at the knee (Ne_k) attenuates in atmosphere as expected from the attenuation length of the EAS particles.

INTRODUCTION

The detailed study of the shape of the break of the size spectrum of EAS (G.V. Kulikov & G.B. Khristiansen 1958) is of main significance to check the different hypothesis about its origin (see e.g. A.D. Erlykin & A.W. Wolfendale 1997). We will therefore discuss the general features of the "knee" as observed by the EAS–TOP array (EAS–TOP Collaboration 1995), with improved statistics and analysis. Observations in different components are in progress (G. Navarra 1996, M. Aglietta et al. 1997).

The EAS–TOP array is located at Campo Imperatore (2000 m a.s.l., 810 g/cm^2 atmospheric depth, National Gran Sasso Laboratories).Its aims are to perform multi-component observations of Extensive Air Showers in the range between 10^{14} and 10^{16} eV, i.e. around the observed "knee". It includes detectors of the electromagnetic (e.m.), muon, hadron, atmospheric Cherenkov light components. Moreover it can run in coincidence with the muon detectors operating in the deep underground Gran Sasso laboratories (MACRO, LVD at muon energy threshold $E_\mu^{th} \approx 1.4$ TeV). Present data have been collected in 256 days of running time (with a 6% inefficiency due to dead time).

THE SHOWER SIZE SPECTRUM

The e.m. detector is made of 35 scintillator modules (10 m^2 each, 4 cm thick, divided into 16 individual units), organized in circles (6 or 7 modules each) of radii r= 50-80 m, interconnected with each other, for trigger and data taking organization. The core location, the slope (s) of the lateral distribution function (*ldf*) and the shower size (Ne) are determined by means of a χ^2 fit in which the particle densities recorded by each module are compared with the theoretical NKG *ldf* (with Moliere radius equal to 100 m). The accuracy in the measurement of the size Ne has been obtained by analyzing showers simulated including all experimental dispersions: for $Ne > 10^5$ we obtain $\Delta Ne/Ne < 15\%$ ($\Delta Ne/Ne < 10\%$ for $Ne > 10^{5.2}$). A detailed description of the event reconstruction and of the experimental setup can be found elsewhere (M. Aglietta et al. 1993).

The shower size expressed in units of *m.i.p.* ($Ne_{m.i.p.}$) is converted to the total number of charged particles (Ne, defined as the number of charged particles with energy $E > 0$ at the depth of the detector following the Greisen formula) by taking into account the transition effect in the scintillators: $Ne/Ne_{m.i.p.} = 1.18$.

The full response of the detector to e.m. cascades has been verified by means of a test performed, with the same scintillators and electronics operating on the field, at a CERN positron beam up to e^+ energies $E_{e^+} = 50$ GeV.

At the purpose of studying the distortions of the shower size spectrum introduced by the event reconstruction we have carried out a detailed simulation that includes the triggering condition, the experimental fluctuations and the analysis procedures. Events are generated on a trial spectrum (I_{mc}) with a unique power law index, then, after the whole data processing, we compare the resulting spectrum (I_{ex}) with the reference one. Thus the function reproducing I_{mc}/I_{ex} vs the shower size is obtained and used to correct each bin content (the values of I_{mc}/I_{ex} changes from 0.8 at $Log(Ne) = 5.3$ to 0.93 at

$Log(Ne) = 6$, and reaches 1 for $Log(Ne) = 6.5$). We thus obtain a measurement of the differential flux where instrumental effects are not larger than 5% in each size bin.

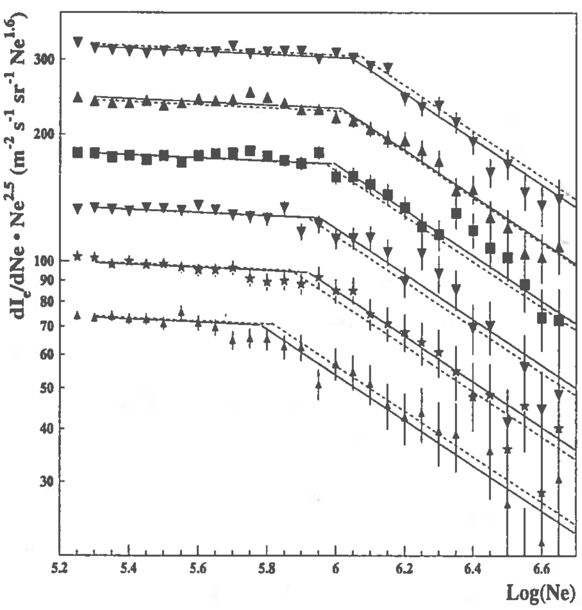

Fig. 1: Differential shower size spectra measured in different zenith angle intervals

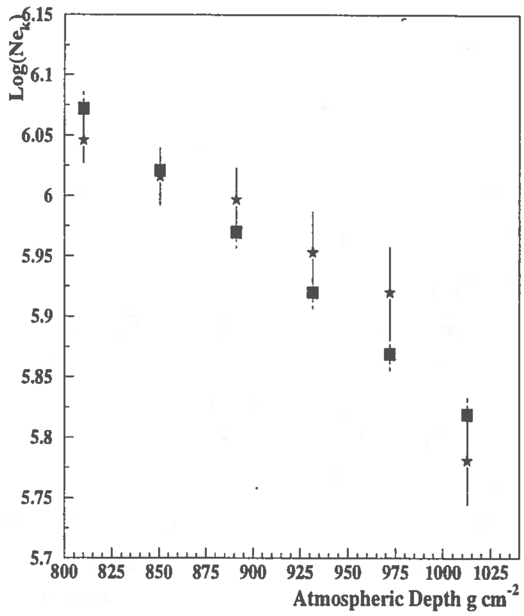

Fig. 2: Shower size value of the knee (Ne_k) measured at different atmospheric depths. Stars represent the values obtained by the first fitting procedure, squares by the second one (see text)

Figure 1 shows the shower size spectra, measured in different zenith angle intervals ($\Delta \sec\theta = 0.05$ each), multiplied by $Ne^{2.5}$ to evidence the change of slope at the knee.

We fit the spectra with the following expression:

$$I_e(Ne) = I_k \cdot (Ne/Ne_k)^{-\gamma_{e_1},\gamma_{e_2}}. \tag{1}$$

At first we calculate, for each zenith angle, the values of γ_{e_1}, γ_{e_2}, I_k and Ne_k. We obtain that the slopes of the spectra are compatible inside the experimental errors. So in the following we will use their weighted means, and their values will no longer be fitted:

$$\gamma_{e_1} = 2.54 \pm 0.02$$
$$\gamma_{e_2} = 3.04 \pm 0.10.$$

This allows to have more detailed informations about the behaviour of Ne_k and I_k vs the atmospheric depth.

The data can be fitted using two different procedures; in the first one the spectra are fitted independently and thus we obtain 6 couples of values of I_k and Ne_k. In the second approach all data together are fitted, leaving as free parameters the size and the primary intensity at the knee of the vertical spectrum and, in the hypothesis that I_k do not depend on the atmospheric depth, the exponential dependence of Ne_k vs x. The two results are shown in figure 1, the first one is represented by solid lines and the second one by dashed lines: inside the experimental errors both fits reproduce the data.

Figure 2 shows the measured dependence of Ne_k on the atmospheric depth (x). The two fits provide compatible results and show the Ne_k exponential decrease with x. Such attenuation factor ($L_k^{exp} = 347.8 \pm 3.2 gcm^{-2}$) is in agreement with the attenuation length of shower particles ($\Lambda =$

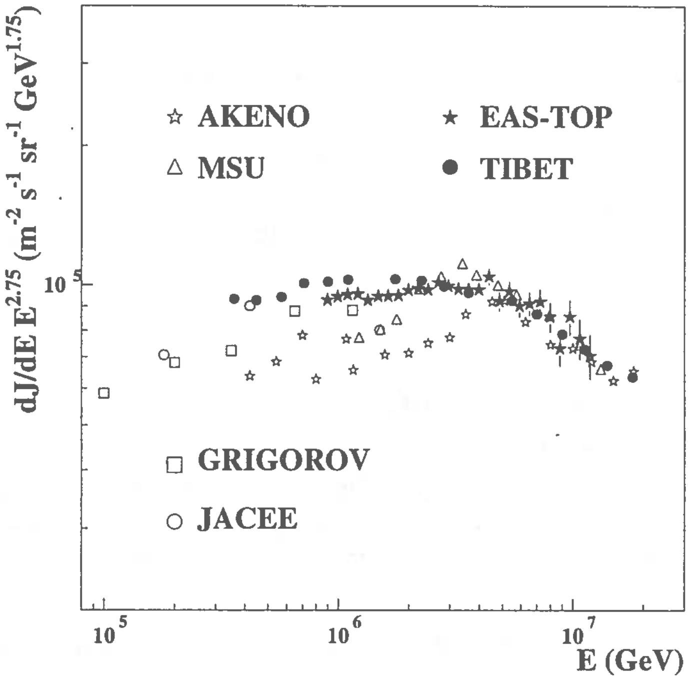

Fig. 3: The all particle spectrum measured at EAS-TOP compared with the results obtained by other experiments operating outside the atmosphere or at earth.

$205 \pm 10.gcm^{-2}$) measured from the constant intensity cut (the expected relation between the two values being $L_k^{exp} \approx 1.6\Lambda$). This is also confirmed by the values of I_k obtained at different x that are nearly constant. Supposing Ne_k constant and I_k depending on x the fitting procedure do not converge.

We thus obtain a quantitative information on the dependence of Ne_k vs x and confirm that the knee of the primary spectrum observed at different atmospheric depths changes as expected from the EAS absorption in atmosphere, showing that the knee is measured at the same primary energy at all atmospheric depths. The result is obtained using the data from a single array, thus overcoming problems due to different calibrations.

Considering only the 3 points around the knee we obtain, from the fits in all angular bins (following the second procedure), χ^2/dof= 1.16. This is an indication that the experimental points are in good agreement with the assumed shape of the knee (i.e. a rather "sharp" one).

THE ALL PARTICLE SPECTRUM

To convert the size spectrum to energy spectrum, complete simulations of the shower development in atmosphere have been performed using the CORSIKA code (Capedevielle et al. 1992). Running the same number of events of fixed primary energy and different masses, the mean values of the shower size and its fluctuations have been obtained at the atmospheric depth of $810gcm^{-2}$. The results for the mean values are parameterized using this expression:

$$Ne = \alpha(A)E_0^{\beta(A)} \tag{2}$$

where the primary energy is expressed in TeV and the parameters α and β are equal to:

$$\alpha(A) = 177.8A^{-0.521} \qquad \beta(A) = 1.107A^{0.035}. \tag{3}$$

The fluctuations for primary protons are:

$$\frac{\sigma(Ne)}{Ne} = 1.378E_0^{-0.235}. \tag{4}$$

Before converting from shower size to primary energy the effect of fluctuations of the EAS development is taken into account. Simulating events over a power law spectrum (again with a unique index) we compare the shower size spectra before and after introducing the fluctuations, obtaining an expression which is used to multiply the experimental result before converting to energy (such factor is 1.15 for $Log(Ne) = 5.5$ and 0.94 at $Log(Ne) = 6.5$). All possible distortions of the primary spectrum are studied without introducing the knee, in order to check that no step of the analysis introduce such feature; and the result is negative.

To convert from shower size to primary energy an effective c.r. primary mass is used:

$$A_{eff}(Ne) = \frac{\sum_i A_i \Phi_i(Ne)}{\sum_i \Phi_i(Ne)} \quad (5)$$

where $\Phi_i = b_i \cdot E_o^{-\gamma_i}$. b_i and γ_i are obtained from the extrapolations of the direct measurements (JACEE Collaboration 1995 and Müller et al. 1991) up to $E_k(A) = Z\ 3 \cdot 10^{15}$ eV, and $\gamma_i \Rightarrow \gamma_i + 0.5$ for $E_o > E_k(A)$ and all nuclear mass groups. The validity of the extrapolation of the lower energy composition data, up to the knee and above (following the Peters Zatsepin model), is supported by the $Ne - N\mu$ data both for $E_\mu > 1.4$ TeV (M. Aglietta et al. MACRO and EAS–TOP colls. 1994) and $E_\mu > 1$ GeV (EAS–TOP Collaboration 1997).

Assuming constant composition above the knee would imply a change of 10% intensity at 10^{16} eV.

The resulting intensity below the knee is $\approx 20\%$ higher than the MSU (Fomin et al. 1991) and Akeno (Nagano et al. 1984) data, and $\approx 10\%$ lower than the recent Tibet ASγ measurements (Amenomori et al. 1996). The data show a good connection with the results obtained by experiments operating on balloon or satellites. At the knee and above, there is a general agreement between all data sets.

REFERENCES

Aglietta, M. et al., EAS–TOP Collaboration, *Nucl. Instr. and Meth.*, **A336**, 310 (1993).

Aglietta, M. et al., MACRO and EAS–TOP Colls., *Phys. Lett.*, **B337**, 376 (1994).

Aglietta, M. et al., EAS–TOP Collaboration, *These Proceedings*, HE 2.1.6 (1997).

Amenomori, M. et al., *Ap. J.*, **461**, 408 (1996).

Capdevielle, J. N. et al., "The Karlsruhe extensive air shower simulation code CORSIKA", KFK Report 4998 (1992).

EAS–TOP Collaboration, *Proc. 24th ICRC*, Rome, **2**, 732 (1995).

EAS–TOP Collaboration, *These Proceedings*, OG 6.1.6 (1997).

Erlykin, A.D & Wolfendale, A.W., *preprint*

Fomin, Yu. A. et al., *Proc. 22nd ICRC*, Dublin, **2**, 85 (1991).

JACEE Collaboration, *Proc. 24rd ICRC*, Rome, **2**, 728 (1995).

Kulikov, G.V. & Khristiansen, G.B., *JEPT*, **35**, 35 (1958)

Müller, D. et al., *Ap.J.*, **374**, 356 (1991).

Nagano, M. et al., *J. Phys. G: Nucl. Phys.*, **10**, 1295 (1984).

SEARCH FOR 30–50 TeV γ RAYS FROM MARKARIAN 421

INFN/AE–97/43
2 Luglio 1997

M.Aglietta[1,2], B.Alessandro[2], P.Antonioli[3], F.Arneodo[4,5], L.Bergamasco[2,6], M.Bertaina[2,6], C.Castagnoli[1,2], A.Castellina[1,2], A.Chiavassa[2,6], G.Cini Castagnoli[2,6], B.D'Ettorre Piazzoli[7], G.Di Sciascio[7], W.Fulgione[1,2], P.Galeotti[2,6], P.L.Ghia[1,2], M.Iacovacci[6], G.Mannocchi[1,2], C.Morello[1,2], G.Navarra[2,6], O.Saavedra[2,6], G.C.Trinchero[1,2], P.Vallania[1,2], S.Vernetto[1,2], C.Vigorito[2,6]

[1] *Istituto di Cosmo-Geofisica del CNR, Torino, Italy*
[2] *Istituto Nazionale di Fisica Nucleare, Torino, Italy*
[3] *Istituto Nazionale di Fisica Nucleare, Bologna, Italy*
[4] *Dipartimento di Fisica dell' Università dell'Aquila, L'Aquila, Italy*
[5] *INFN Laboratori Nazionali del Gran Sasso, Assergi (AQ), Italy*
[6] *Dipartimento di Fisica Generale dell' Università, Torino, Italy*
[7] *Dipartimento di Scienze Fisiche dell' Università and INFN, Napoli, Italy*

ABSTRACT

We present a study of Markarian 421 (observed in γ-rays at HE and VHE energies by the EGRET and Whipple telescopes respectively) performed through the e.m. detector of EAS-TOP at primary energies 30-50 TeV and 90 TeV. A straight power law extrapolation of the EGRET-Whipple spectrum up to $E_0 \approx 10^{15}$ eV is excluded with good confidence level, as expected from the absorption of VHE γ-rays by the 2.7K microwave background radiation. An indication, although weak, of a steepening of the spectrum with respect to such extrapolation at γ-ray energies lower than expected from the 2.7K cutoff is derived. This could be due either to a break in the source spectrum or to the intergalactic absorption of γ-rays by a radiation of wavelength $\lambda \approx 10\ \mu$m, whose presence is predicted within some models.

INTRODUCTION

The measurement of the very high energy tail of the AGNs γ-ray spectrum is of utmost interest for the study both of the physics of the sources and of the intergalactic low energy background radiation - the cosmic microwave background at 2.7K (CMBR) (Gould and Schreder, 1966) and the intergalactic infrared radiation fields (Stecker et al., 1992, Stecker and De Jager, 1993)

The best candidate for such a study is represented by Markarian 421, observed with high statistical significance (and therefore with well measured fluxes) both in the GeV energy range by EGRET (Lin et al., 1992) and at TeV by the Whipple ground based atmospheric Cherenkov light detector (Punch et al., 1992, Mohanty et al., 1993, Krennrich et al. 1997). In fact a single power law spectrum fits well the data over the whole energy range, and the source distance ($z \approx 0.031$) is such that the intergalactic absorption is not too severe, so that ground based EAS arrays could have enough sensitivity to detect the expected extrapolated fluxes. At γ-ray energies above the Cherenkov measurements, upper limits have been reported at $\approx$ 10 TeV by the Tibet experiment (Amenomori et al., 1994), and above 50 and 100 TeV by the Cygnus (Alexandreas et al., 1993) and CASA-MIA arrays (Catanese et al., 1997).

In the present note we report on the observations performed by the EAS-TOP array (preliminary results are reported in Aglietta et al., 1995a) which is sensitive around 90 TeV and, through lower energy events, in the 30-50 TeV range, i.e. the regions around and below the CMBR cutoff, interesting for the possible intergalactic absorption of VHE γ-rays by infrared radiation of wavelength $\approx 10\ \mu$m.

THE EXPERIMENT AND THE DATA

The EAS-TOP array is located at Campo Imperatore (2005 m a.s.l., INFN National Gran Sasso Laboratories, lat. 42.5° N, long. 13.5° E). The electromagnetic detector (Aglietta et al., 1988, 1993) consists of 35 modules of scintillator 10 m^2 each, spread over an area of $\approx 10^5$ m^2.

Different selection criteria, based on the number of triggered modules, core location, shower size are applied to the data in order to investigate different primary energies. In the present analysis we are interested in events with $\geq$4 modules fired, without core location (TR_0), and $\geq$7 modules fired and core located inside the edges of the array (TR_1 events). The typical triggering primary energies in the angular window $\theta \leq 40^o$ are 30 and 90 TeV. The angular resolutions are respectively σ_θ=2.5° (taking into account the uncertainty in core location) and σ_θ=0.83° $\pm$ 0.10° (which includes systematic effects and is obtained by the measurement of the shape of the Moon shadow on the flux of primary cosmic rays, Aglietta et al., 1991, 1995b).

The search is performed by means of the ON-OFF technique (details about the procedure, a study of the background stability, the calculations of the array effective area, energy thresholds and reported upper limits are discussed in Aglietta et al., 1995a, 1995b). The number of counts from the source direction (ON) is compared with the number of counts from six OFF-source cells located in the same declination band and next to the ON source bin. The used angular bins are: $\Delta\delta = 1.5^o$ (with efficiency from a point source $\epsilon = 0.9$) for TR_1 and $\Delta\delta = 4.0^o$ for TR_0 ($\epsilon = 0.7$), while $\Delta\alpha = \Delta\delta/\cos\delta$=1.9^0 and 5.1^0 respectively.

Data have been collected between 1992 and 1997 for a total observation time $T_{obs} = 2.95 \cdot 10^7 s$ both for the ON and the OFF sources.

RESULTS AND CONCLUSIONS

The experimental data are compared with the expectations from the source spectrum fitting the EGRET-Whipple data:

$$\frac{dN}{dE} = (1.02 \pm 0.14)10^{-11}\ E^{-2.06\pm0.04}\ \gamma\ cm^{-2}s^{-1}TeV^{-1} \qquad (1)$$

Due to the known source variability, at least over short times, some care should be taken in assuming the emission to be stable over the long observation time of EAS-TOP. Indeed the EGRET and Whipple observations are not continuous; however, the good alignment of the two measurements on the quoted power law guarantees to some extent the stability of the spectrum. The error in the flux when extrapolated to the primary energies of interest in the EAS-TOP measurements are expected to be $\leq 20\%$.

The extrapolation of expression (1) is performed:

a) as a single power law spectrum up to $10^{15} eV$, and

b) as in a), but including the absorption from the CMBR (see e.g. the calculations reported in Catanese et al., 1997).

The response of TR_0 and TR_1 events to the γ-ray spectra derived from the two hypothesis a) and b) is shown in fig. 1. and 2. The number of expected and measured events, for the two trigger conditions, are:

expected source contribution:

without CMBR cutoff (a): TR_0: S_0 = 7,440; TR_1: S_1 = 1,181;

with CMBR cutoff (b): TR_0: S_0 = 3,372; TR_1: S_1 = 331.

observations:

TR_0: ON = 11,597,932; <OFF> = 11,599,310;

TR_1: ON = 125,148; <OFF> = 125,559.

Comparing these observed rates (which show a good compatibility - within 1 s.d.- between ON and <OFF> counts) with the expectations from the two hypothesis (a) and (b), we conclude:

(i) concerning the straight power law extrapolation of the spectrum (a) and considering TR_0 events,

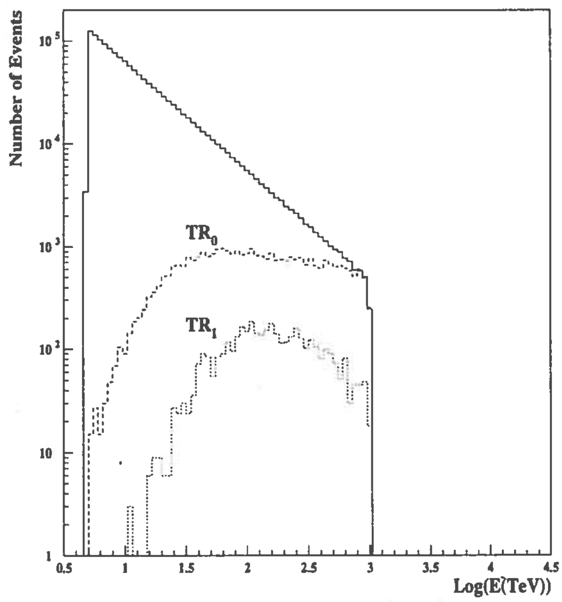

Fig. 1: Response of trigger TR_0 and TR_1 to the source spectra derived under hypothesis a)

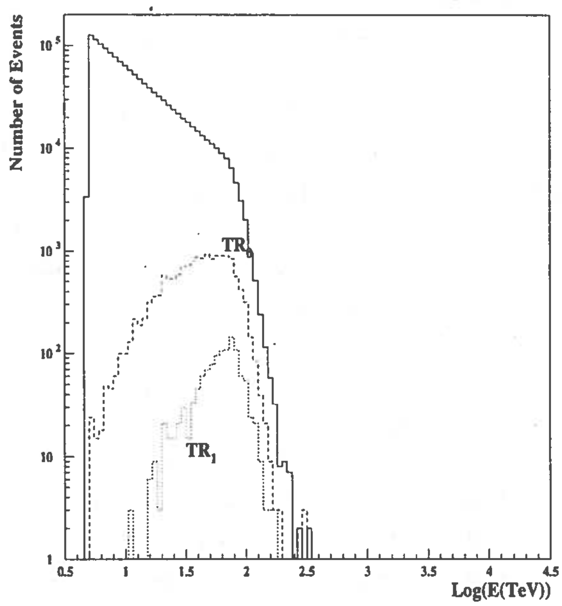

Fig. 2: Response of trigger TR_0 and TR_1 to the source spectra derived under hypothesis b)

the probability of observing $n_{0,a} \leq 11,597,932$ events against an expectation of $(11,599,310+7,440)$ is $P_0^{pl} = 8.4 \times 10^{-3}$ (corresponding to 2.4 s.d.), the uncertainty of <OFF> being included. Hypothesis (a) is also excluded by TR_1 events, for which the probability of observing $n_{1,a} \leq 125,148$ events against an expectation of $(125,559 + 1,181)$ is $P_1^{pl} = 2. \times 10^{-5}$ (corresponding to 4.1 s.d.).

(ii) Concerning hypothesis (b), i.e. including the CMBR cutoff, and considering TR_0 events, the probability of observing $n_{0,b} \leq 11,597,932$ events against an expectation of $(11,599,310\ +3,372)$ events is $P_0^{pl+CMBR} = 10^{-1}$ (corresponding to 1.3 s.d.). Moreover, from TR_1 events, the probability of observing $n_{1,b} \leq 125,148$ events against an expectation of $(125,559 + 331)$ is $P_1^{pl+CMBR} = 3. \cdot 10^{-2}$ (corresponding to 1.9 s.d.). The significance of these limits (even if combined) is certainly not compelling, also in view of the quoted uncertainties in the source flux. However, these first data in this energy range provide an indication - although weak - of a break in the Markarian 421 spectrum at γ-ray energies $E_0 \approx 10$ TeV, or of the presence of a $\lambda \approx 10\ \mu$m infrared radiation in the intergalactic space, as predicted within some models of the galactic infrared emission (see e.g. Stecker 1992, 1993).

ACKNOWLEDGEMENTS
Stimulating discussions with V.S. Berezinsky are gratefully acknowledged.

REFERENCES

Aglietta M. et al., Nucl. Instr. and Meth., A277, 23 (1988)
Aglietta M. et al., Proc. 22nd ICRC, 2, 708 (1991)
Aglietta M. et al., Nucl. Instr. and Meth., A336. 310 (1993)
Aglietta M. et al., Proc. 24th ICRC, 2, 421 (1995a)
Aglietta M. et al., Astroparticle Phys., 3, 1 (1995b)
Alexandreas D.E. et al., Ap. J., 418, 832 (1993)
Amenomori M. et al., Ap. J., 429, 634 (1994)
Catanese M. et al., Ap. J., 469, 572 (1997)
Gould R.J. and Schreder S., Phys. Rev. Lett., 16, 252 (1966)
Krennrich F. et al., Ap. J., in press (1997)
Lin Y.C. et al., Ap. J., 401, L61 (1992)
Mohanty G. et al., Proc. 23rd ICRC, 1, 440 (1993)
Punch M. et al., Nature, 358, 477 (1992)
Stecker F.W. et al., Ap. J., 390, L49 (1992)
Stecker F.W. and De Jager O.C., Ap. J., 415, L71 (1993)